

Short communication

Studies of heteropoly acid/polyvinylidenedifluoride–hexafluoropropylene composite membranes and implication for the use of heteropoly acids as the proton conducting component in a fuel cell membrane

Jennifer L. Malers^{a,c}, Mary-Ann Sweikart^{a,c}, James L. Horan^b,
John A. Turner^{c,*}, Andrew M. Herring^{a,*}

^a Department of Chemical Engineering, Colorado School of Mines, Golden, CO 80401, United States

^b Department of Chemistry and Geochemistry, Colorado School of Mines, Golden, CO 80401, United States

^c Hydrogen Technologies and Systems Center, National Renewable Energy Laboratory, Golden, CO 80401, United States

Received 6 January 2007; received in revised form 10 February 2007; accepted 12 February 2007

Available online 17 February 2007

Abstract

Complete polarization curves for a number of heteropoly acids (HPAs), $H_3PW_{12}O_{40}$, $\alpha-H_3P_2W_{18}O_{62}$, $H_6P_2W_{21}O_{71}$, and $H_6As_2W_{21}O_{69}$ as the only proton conducting component are presented for the first time. Both thin pellets of HPA and composite membranes of 1:1 (w/w) of HPA and polyvinylidenedifluoride–hexafluoropropylene (PVDF–HFP) are investigated. Although the pellets are somewhat variable, the HPA phase changes can be observed by electrochemistry and these materials show promise for solid acid fuel cell performance at $>200^\circ C$. The high proton conductivities reported for HPAs at RT are demonstrated in fuel cells using HPA/PVDF–HFP composites with limiting current densities as high as $1.6 A cm^{-2}$ using dry O_2 and H_2 . Moderate fuel cell activity is demonstrated for $\alpha-H_3PW_{18}O_{62}$ at $120^\circ C$ and 25%RH. Unfortunately all of the materials studied were somewhat porous and the open circuit potentials observed were somewhat low. We were also able to show that an HPA fuel cell could be shorted by reduction of the HPA to a heteropoly blue under exceptional circumstances.

© 2007 Elsevier B.V. All rights reserved.

Keywords: Proton exchange membrane; Heteropoly acid; Polyvinylidenedifluoride; Proton conduction

1. Introduction

The proton exchange membrane (PEM) fuel cell is a very promising electrochemical energy conversion device. PEM fuel cells are not widely commercially available as they are still too expensive, suffer from durability issues, are limited in operating temperatures to $<100^\circ C$, and require that the inlet gases be fully humidified. Current state of the art PEMs are comprised of perfluoro sulfonic acid (PFSA) ionomers such as Nafion[®] [1]. To maintain practical proton conduction, PFSA ionomers must be fully hydrated. This necessitates hydrating the inlet gases of the fuel cell, which restricts the amount of reactant gases

that can be delivered to the fuel cell. This also makes operation above $100^\circ C$ impractical due to the need to use excessive pressure, and the external humidification equipment introduces parasitic loads, increasing system complexity. The use of a PEM that did not need to be hydrated and could be operated above $100^\circ C$ would dramatically simplify PEM fuel cell operation, allow better heat transfer (enabling combined heat and power applications and the use of conventional vehicle technology), and facilitate the use of reformed hydrogen from hydrocarbons with higher levels of CO thereby simplifying the complexity of the reformer and reducing overall system cost. While a large number of studies have appeared modifying PFSA ionomers with additives to create improved composite membranes, none of these materials performs adequately under dry or elevated temperature, $>100^\circ C$, conditions [2]. There is, therefore, a need to investigate proton conducting materials not based on hydrated sulfonic acids if we are to develop PEMs for dry and/or higher temperature operating conditions.

* Corresponding author. Tel.: +1 303 384 2082; fax: +1 303 273 3730.

E-mail addresses: john.turner@NREL.gov (J.A. Turner),

herring@mines.edu (A.M. Herring).

¹ Tel.: +1 303 275 4270; Fax: +1 303 275 2905.

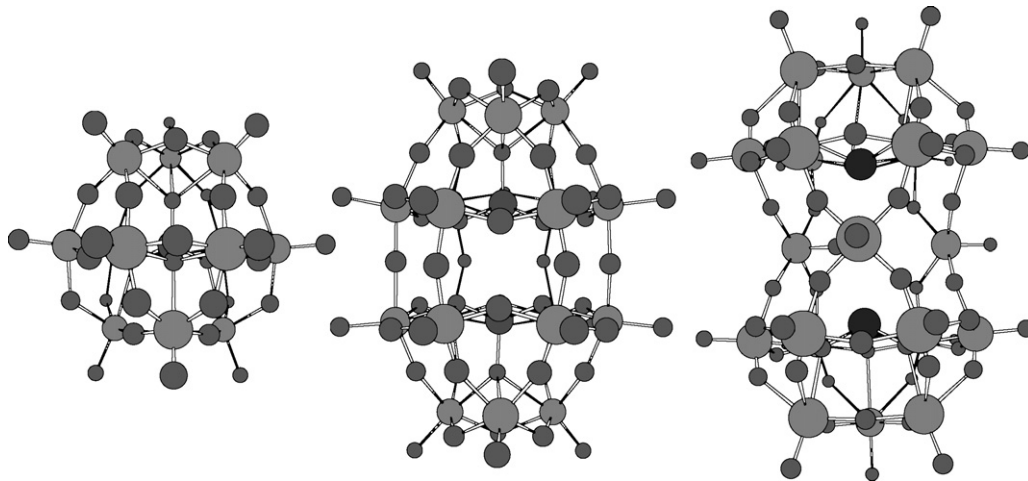


Fig. 1. Structures of heteropoly acids, from left Keggin, Wells–Dawson and $[\text{As}_2\text{W}_{21}\text{O}_{69}]^{6-}$.

The heteropoly acids (HPAs), a subset of the well-known inorganic metal oxides known as polyoxometallates [3,4], are class of an intriguing set of solid state proton conducting super acids. HPAs based on the Keggin structure have some of the highest reported solid-state proton conductivities at room temperature [5] and proton transport in these materials has been extensively studied [6–12]. The HPAs are becoming an increasingly popular proton conducting additives in ionomer composite membranes for use under dry and/or elevated temperature conditions [2]. Owing to their solubility in water, attempts to measure fuel cell performance in the solid state for systems in which the HPA is the only proton conductor are limited and unpromising [13,14]. A fuel cell has been developed based on using an aqueous HPA electrolyte [15,16]. As Pt rapidly catalyzes the reduction of the HPA at the anode to the electrically conducting heteropoly blue in solution these fuel cells must use a circulating electrolyte to reoxidize the heteropoly blue to the HPA.

Data obtained in our laboratory suggests that proton self-diffusion coefficients of many HPA continue to increase above 100 °C, although not all the protons may be available for proton conduction [17]. As a number of these HPAs were available to us we decided to obtain fuel cell performance data for a representative class as the sole proton conducting component in membranes using polyvinylidenedifluoride–hexafluoropropylene (PVDF–HFP) as the inert binder. These membranes are not intended to be for use in practical fuel cells rather the intention is to demonstrate that pure HPA can act as the ionomer in an operating fuel cell. The fuel cells were run with dry inlet gases or at elevated temperatures to minimize dissolution of the HPA.

The HPAs chosen were of varying structure and included Keggin, Wells–Dawson and elongated structures based on the Wells–Dawson structure. HPAs of the Keggin structure and the Wells–Dawson structure are the most commonly studied. The Keggin anion, $[\text{X}^{+n}\text{M}_{12}\text{O}_{40}]^{(8-n)-}$ (where M commonly = W or Mo, and X can be almost any cation), has a structure with T_d symmetry and is composed of a central heteroatom surrounded by four groups of three M–O octahedra (Fig. 1). The related Wells–Dawson structure $[(\text{X}^{+n})_2\text{M}_{12}\text{O}_{40}]^{(16-2n)-}$ (M = W or

Mo) is closely related to the Keggin ion and may be imagined to consist of two Keggin ions with one face of three M–O octahedra removed and then joined together (Fig. 1). The Wells–Dawson structure can be imagined to be further elongated by the addition of a belt of three additional W–O octahedral between the two Keggin subunits as in $[\text{As}_2\text{W}_{21}\text{O}_{69}]^{6-}$ where the two opposing As lone pairs repel each other and the related $[\text{P}_2\text{W}_{21}\text{O}_{71}]^{6-}$ which is formed from the condensation of two $[\text{PW}_{11}\text{O}_{38}]^{8-}$ anions derived from the Keggin anion by removal of one W–O octahedral (Fig. 1).

2. Experimental

2.1. Materials

The HPAs were either obtained commercially and used as received: $\text{H}_3\text{PW}_{12}\text{O}_{40}$ (HPW) (Aldrich); or were prepared by literature methods [18,19] and purified by recrystallization followed by conversion to the free acid via the ether adduct: $\alpha\text{-H}_3\text{P}_2\text{W}_{18}\text{O}_{62}$ (HP2W18); $\text{H}_6\text{P}_2\text{W}_{21}\text{O}_{71}$ (HP2W21); $\text{H}_6\text{As}_2\text{W}_{21}\text{O}_{69}$ (HAS2W21). All HPA were dried and stored in an oven at 115 °C prior to use. PVDF–HFP, $M_w \approx 455,000$, $M_n \approx 110,000$ was obtained commercially (Aldrich).

2.2. Membrane electrode assembly (MEA) fabrication

Two millimeter thick pellets of pure HPA were obtained by pressing 5 g of the material in a 5 cm diameter pellet die at 10,000 psi in a Craver Press, with an A-6 solid polymer electrolyte electrode Los Alamos type (ELAT) V2.1 hand fabricated, single sided coatings with 0.5 mg cm^{-2} 20% Pt on carbon (DeNora) on either side. For the PVDF–HFP/HPA membranes, PVDF–HFP (1 g) was dissolved in HPLC grade refluxing acetone (30 cm^3) and an equal weight of the HPA added. The solution was cast on a glass plate and allowed to dry. Thinner membranes were obtained by spin coating. Thickness measurements were made at various points over the membrane with a digital micrometer and average values are reported. MEAs were fabricated by pressing at 10,000 psi and room tempera-

ture, ELATs (as described above) hand painted with an acetone solution of HPA (0.25 g in 2 cm³) onto the membranes.

2.3. Fuel cell testing

Gases were metered by a modular gas handling system, set with 30 psi back pressure (Lynntech Industry Inc., GMET/H) and were usually dry unless humidified with a bubble humidifier (Lynntech Industry Inc., BH), and were fed via heated transfer lines to the single fuel cell hardware. The fuel cell hardware (Fuel Cell Technologies Inc., 5SCH) has an active area of 5 cm² as serpentine flow fields in Poco carbon blocks which were heated as needed. Polarization curves were measured with a MSTAT4+ multi-potentiostat (Arbin Instruments, Austin, TX, BT 4+) or by an electronic load and the entire system was controlled with FC Power software (Lynntech Industry Inc.). Polarization curves were obtained at constant flow of dry (unless otherwise stated) H₂ and O₂, typically at 0.5 l min⁻¹. The total resistance of the cell was measured with a multimeter across the cell to determine if the cell was electrically short circuited.

3. Results and discussion

3.1. Pure HPA pellets

Powdered dried HPAs may be pressed under pressure into contiguous transparent pellets. By carefully placing an even layer of powdered dried HPA between two ELAT electrodes a MEA may be fabricated by pressing the whole assembly at 10,000 psi. Five grams of HPA will often yield a 2 mm thick pellet of sufficient integrity for experimental use. Unfortunately as this is literally a pressed crystalline material we do not expect the MEA to be particularly robust. So not only do we observe low OCV due to a fair amount of reactant gas cross-over, but, many fabricated MEAs of these pure materials are not of sufficient quality for testing. A typical polarization curve for this type of MEA under dry O₂ and H₂ at RT is shown in Fig. 2. The open circuit voltage (OCV) is rather low, 0.7 V, although we have observed OCVs in these systems as high as 0.8 V. A respectable

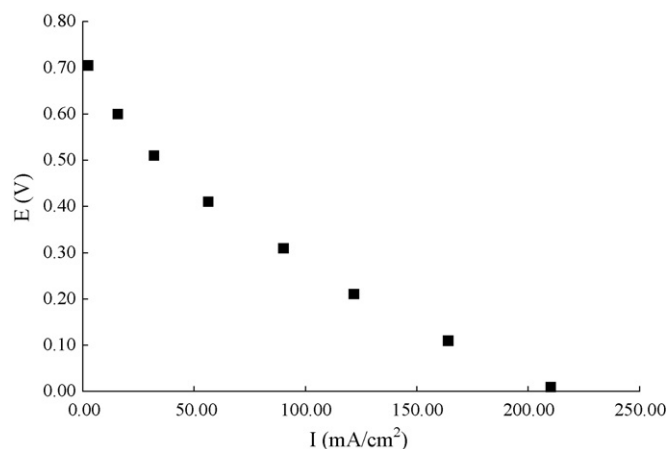


Fig. 2. Polarization curves for 1:1 HPW/PVDF pellets using an inlet RH of 0%, H₂ and O₂ at 0.5 l min⁻¹ at RT.

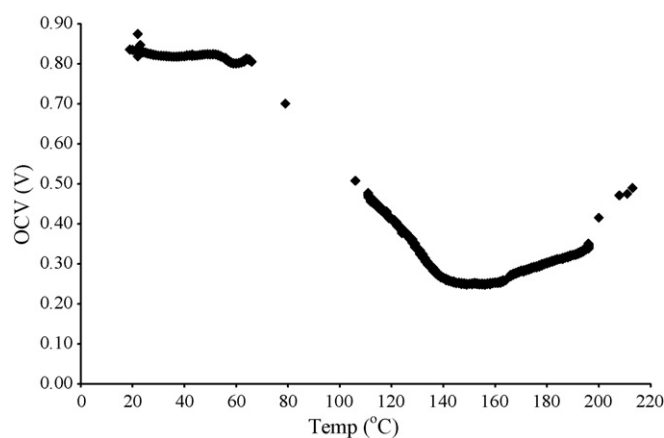


Fig. 3. OCV vs. temperature for 1:1 HPW/PVDF pellets using an inlet RH of 0%, H₂ and O₂ at 0.5 l min⁻¹ at RT.

limiting current density (LCD) of 200 mA cm⁻² is obtained for this cell indicating that proton conduction is occurring and the cell is operating as a fuel cell. LCDs as high as 400 mA cm⁻² may be obtained in these systems.

As HPAs are heated above RT they undergo a number of crystallographic phase changes as they loose most, but not all of the waters associated with the anions until a limiting hydration state is reached. HPW has *ca.* 23H₂O at room temperature, a well-defined limited hydration state with six waters of cubic structure, and at least two other phases which are transversed in going from RT to above 100 °C [20]. This is seen when following the OCV with temperature as the cell is heated (Fig. 3). Transitions are seen at both 52 and 65 °C before the OCV degrades as the limiting hexaqua forms. Whilst the OCV only fluctuate mildly during these phase changes the LCD of the cell at 60 and 80 °C falls to 65 and 25 mA cm⁻², respectively, from polarization data, not shown. In this crystalline phase the water molecules are tightly bound and most of the protons cannot move. Our attempts to obtain polarization curves at or slightly above 100 °C have failed. However, as the temperature of the cell is raised above 165 °C the OCV again increases. Polarization of the cell at these much higher temperatures does result in a response, albeit in μ A, with the LCD of the cell *ca.* 0.5 mA cm⁻² at temperatures >200 °C, data not shown. This is very similar behavior to what we observed in HPA composite membranes with high temperature epoxies [21]. Obviously, proper optimization of these materials would result in a high temperature fuel cell of similar performance to other solid acids [22]. We are not, however, proposing that the HPA undergo a superprotonic phase change, simply that the activation barrier for proton transport has been overcome.

3.2. PVDF–HFP/HPA composite membranes

A more reasonable approach to studying the fuel cell performance of HPA is to suspend it in an inert polymer. PVDF–HFP was chosen as it is inert and not an ionomer, additionally, this co-polymer was designed by the battery industry for greater processability. PVDF–HFP and HPA both conveniently dissolve in hot acetone and so it was relatively easy to prepare casting solu-

Table 1
Polarization data for 1:1 HPW/PVDF–HFP membranes of various thicknesses at an inlet RH of 0%, H₂ and O₂ at 0.51 min⁻¹

Thickness (μm)	OCV (V)	Current at 0.2 V (mA cm ⁻²)
1200	0.90	7
70	0.77	145
30	0.65	1350

tions from these components. Our initial attempts to produce hand spreads resulted in somewhat thick membranes, but we were able to routinely produce films <50 μm by spin coating the casting solution.

We have assumed in the preceding discussion that low OCV observed in these cells is due to gas cross-over. However, the low OCV could be due to concentration effect due to poor interfacial resistance or the HPA overwhelming the Pt catalyst and catalyzing the 2e⁻ reduction of oxygen to peroxide, $E^0 = 0.695$ V, rather than the 4e⁻ reduction to water, $E^0 = 1.229$ V. When HPA are used as the fuel cell cathode catalyst, the fuel cell OCV is almost always 0.7 V indicating strongly that the HPA are good 2e⁻ oxygen reduction catalysts [23,24]. Despite this, it appears that the low OCV in these cells is due to cross-over. In a series of HPW/PVDF–HFP MEAs of differing thickness (Table 1) OCV clearly drops as membrane thickness decreases, which is very strong evidence for increased cross-over as the concentration of HPA and method of MEA fabrication are constant. Similarly for a series of MEAs composed of HAs2W21/PVDF–HFP the OCV (Fig. 4) OCV clearly decreases with membrane thickness. Neither of these correlations is linear.

Excitingly the LCD for the thinnest HPW/PVDF–HFP MEA at RT with no inlet humidification is 1.3 A cm⁻² (Table 1, Fig. 5). This observation is certainly in keeping with the high RT proton conductivity measured for HPW and is of the same order of magnitude as would be obtained for a MEA of a PFSA ionomer. Unfortunately the HPA is water soluble and the water produced by the cell both electrochemically and chemically from cross-over still dissolves the HPA. This results in a degradation in performance when fuel cells of this material are run at high current density. In Fig. 5, we can see that the LCD of the MEA degrades

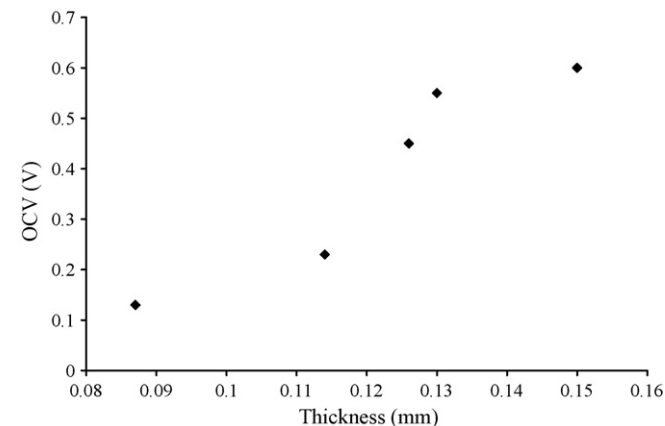


Fig. 4. OCV vs. membrane thickness for a series of 1:1 Has2W21/PVDF pellets using an inlet RH of 0%, H₂ and O₂ at 0.51 min⁻¹ at RT.

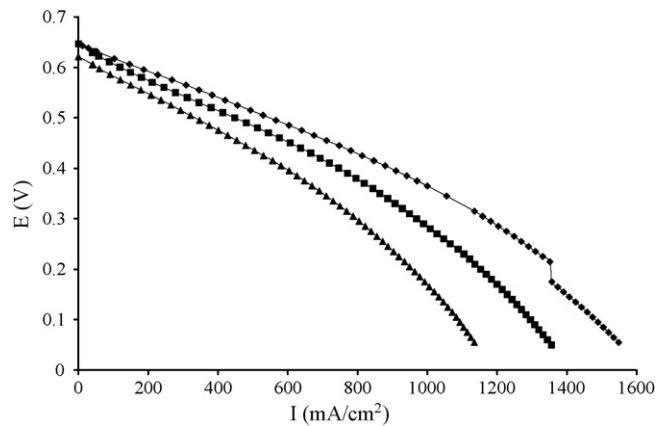


Fig. 5. 1st (◆) 2nd (■) and 3rd (▲) polarization curves for a 1:1 HPW/PVDF–HFP membrane, 30 μm, using an inlet RH of 0%, H₂ and O₂ at 0.51 min⁻¹ at RT.

by ~200 mA cm⁻² with each successive polarization curve as the ionomer is washed from the cell by the product water.

HPA of varying structure can behave as reasonable PEM fuel cell ionomers at room temperature using dry gases. Polarization curves are shown in Fig. 6 for a number of HPA/PVDF–HFP composite MEAs of similar thickness. All these materials clearly have high proton conductivities as the LCDs are all in the 100 s of mA cm⁻². HPW has the most promising OCV whereas the two larger P heteroatom materials HP2W18 and HP2W21 appear to have superior LCD performance. Unfortunately polarization curves could not be obtained for any of these MEAs at >100 °C, even when 25%RH was introduced. The exception was the Wells–Dawson HPA, HP2W18, which at 120 °C and 25%RH shows modest fuel cell activity (Fig. 7). This HPA as an OCV of 0.7 V and a LCD of 5.5 mA cm⁻². We attempted to measure proton conductivities of these MEAs by cyclic voltammetry using four Pt electrodes in H₂, but almost all of the MEAs reduced and short circuited, see further discussion below. However, for the HP2W18/PVDF–HFP MEA at 120 °C and 25%RH, this proton pump experiment was successful and a value of $\sigma = 0.032$ S cm⁻¹ was obtained which is encouraging.

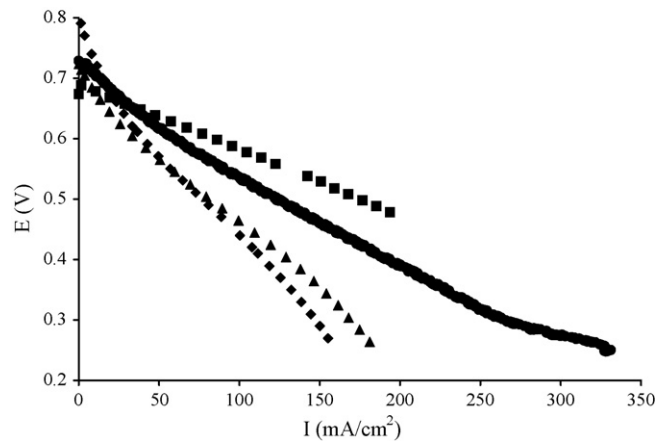


Fig. 6. Polarization curves for a 1:1 HPA/PVDF–HFP membrane, using an inlet RH of 0%, H₂ and O₂ at 0.51 min⁻¹, at RT; ◆, HPW, 155 μm; ■, HP2W18, 100 μm; ●, 119 μm HP2W21; ▲, HAs2W21, 295 μm.

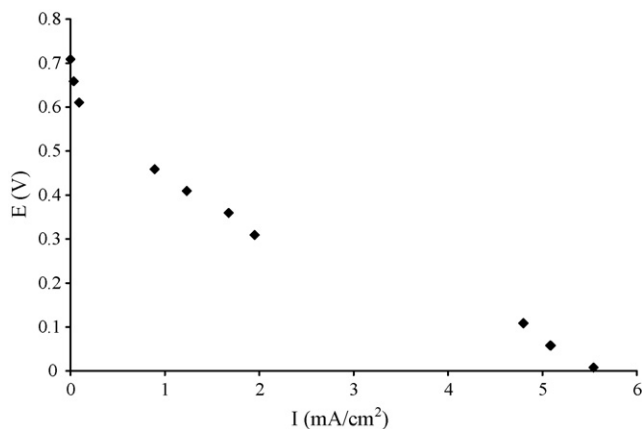


Fig. 7. Polarization curve for 1:1 HP2W18/PVDF-HFP membrane, 119 μm , using an inlet RH of 25%, H_2 and O_2 at 0.51 min^{-1} at 120°C .

Our inability in measuring the proton conductivity by the proton pump method caused us to investigate under what conditions an HPA fuel cell could be shorted by reduction of the HPA to the electronically conducting heteropoly blue. To date we have not shorted a fuel cell in which the membrane is composed of a PFSA-ionomer/HPA composite [25,26]. HPA are reduced by H_2 especially in the presence of a catalyst such as Pt and this is the Achilles heel of the aqueous based HPA fuel cell [16,27]. Two sets of MEAs were studied, one using a HPW/PVDF-HFP membrane and the other a HAS2W21/PVDF-HFP membrane. The O_2 flow rate was increased to 11 min^{-1} and the H_2 flow incrementally increased up from 0.11 min^{-1} . As can be seen from Figs. 8 and 9 both the OCV and the cell resistance slowly decrease as the H_2 flow rate is increased to 0.51 min^{-1} . However, when the flow rate is increased to 0.751 min^{-1} both the OCV and the cell resistance fall precipitously. We believe that as the flow rate of H_2 and O_2 approach the same value at these high flow rates, the smaller H_2 is fully saturating the MEA and as these MEAs are relatively thin, the HPA has become reduced to a heteropoly blue and the cell has electrically shorted.

In the above experiments the water produced from the fuel cell was collected and quantified. As the O_2 flow rate was

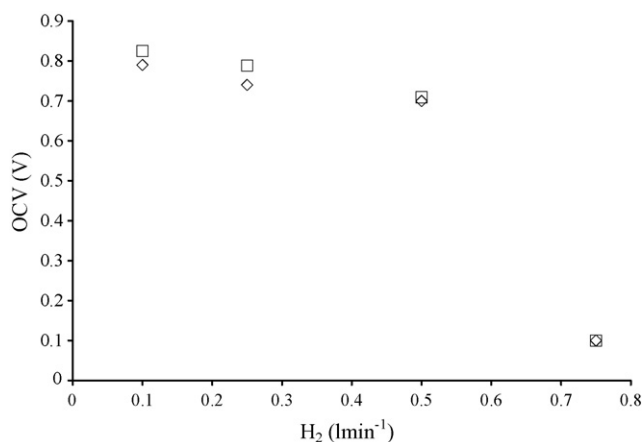


Fig. 8. OCV for a 1:1 HPW/PVDF-HFP, $157 \mu\text{m}$ (\diamond) and a 1:1 HP2W21A/PVDF-HFP, $75 \mu\text{m}$ (\square) vs. H_2 flow rate, with O_2 at 11 min^{-1} , RT.

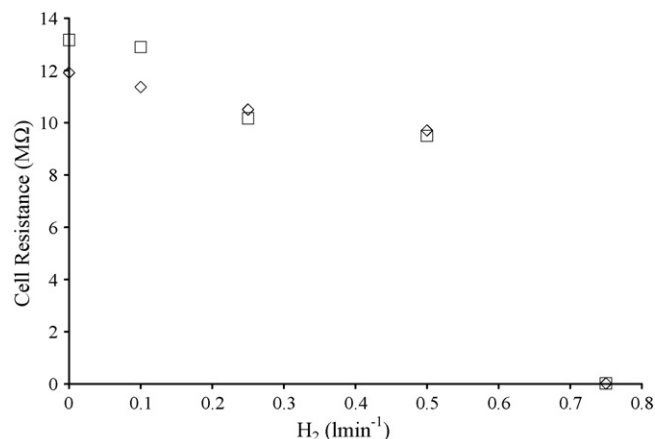


Fig. 9. Cell resistance for a 1:1 HPW/PVDF-HFP, $157 \mu\text{m}$ (\diamond) and a 1:1 HP2W21A/PVDF-HFP, $75 \mu\text{m}$ (\square) vs. H_2 flow rate, with O_2 at 11 min^{-1} , RT.

so much higher, the largest amount of water was produced at the anode as some O_2 was clearly being pushed through the membrane and reacting with H_2 at the anode. The total current produced during the experiment was obtained by integrating under the polarization curve by the trapezoid method. From this we could calculate the amount of water produced electrochemically and by subtraction from the water produced by the cell the water produced chemically via cross-over. For both cells it was shown that $1\text{--}3 \text{ ml min}^{-1}$ of O_2 was crossing over from the cathode, again showing not surprisingly that these membranes were quite porous. This is not surprising as these membranes are simply crystalline materials embedded in a polymer matrix. The major deficiency in OCV is caused by cross-over and not by electronic, catalytic or concentration effects.

4. Conclusions

We have demonstrated that the high proton conductivities reported in the literature for HPA can be translated in to impressive currents in PEM fuel cells at RT with no external humidification. However, HPA on their own do not have sufficient mobility of their protons for fuel cell temperature operation at *ca.* 100°C . Intriguingly these materials may have application for use as high temperature PEMs at *ca.* 200°C , although we are quick to point out that we only investigated a small subset of the many structures available. One HPA, HP2W18, did show moderate activity at 120°C with the application of some humidity.

All of the membranes studied were certainly not optimized and suffered from porosity issues. We were able to take advantage of this to show that a pure HPA membrane could be shorted by reduction of the HPA to the heteropoly blue.

Acknowledgement

This work was funded by a science initiative grant, DE-FC02-00CH11088, from the US Department of Energy.

References

- [1] A.M. Herring, in: S. Lee (Ed.), *Encyclopedia of Chemical Processing*, Marcel Dekker, New York, 2006, pp. 1085–1097.
- [2] A.M. Herring, *Polym. Rev.* 46 (3) (2006) 245.
- [3] M.T. Pope, A. Müller (Eds.), *Polyoxometalate Chemistry: From Topology via Self-Assembly to Applications*, Kluwer Academic Publishers, Dordrecht, 2001.
- [4] M.T. Pope, *Heteropoly and Isopoly Oxometalates*, Springer Verlag, New York, 1983.
- [5] O. Nakamura, T. Kodama, I. Ogino, Y. Miyake, *Chem. Lett.* 1 (1979) 17.
- [6] S.F. Dec, A.M. Herring, *J. Phys. Chem., B* 108 (33) (2004) 12339.
- [7] R.C.T. Slade, M.J. Omana, *Solid State Ionics* 58 (3–4) (1992) 195.
- [8] R.C.T. Slade, H.A. Pressman, E. Skou, *Solid State Ionics* 38 (3–4) (1990) 207.
- [9] R.C.T. Slade, J. Barker, H.A. Pressman, J.H. Strange, *Solid State Ionics* 28–30 (1988) 594.
- [10] H.A. Pressman, R.C.T. Slade, *Chem. Phys. Lett.* 151 (4–5) (1988) 354.
- [11] K.D. Kreuer, M. Hampele, K. Dolde, A. Rabenau, *Solid State Ionics* 28–30 (1) (1988) 589.
- [12] A. Hardwick, P.G. Dickens, R.C.T. Slade, *Solid State Ionics* 13 (4) (1984) 345.
- [13] O. Nakamura, *Prog. Batteries Sol. Cells* 4 (1982) 230.
- [14] P. Staiti, S. Hocevar, N. Giordano, *Int. J. Hydrogen Energy* 22 (8) (1997) 809.
- [15] N. Giordano, P. Staiti, A.S. Arico, E. Passalacqua, L. Abate, S. Hocevar, *Electrochim. Acta* 42 (11) (1997) 1645.
- [16] N. Giordano, P. Staiti, S. Hocevar, A.S. Arico, *Electrochim. Acta* 41 (3) (1996) 397.
- [17] F. Meng, J.L. Horan, J.L. Malers, S.F. Dec, J.A. Turner, A.M. Herring, *Div. Fuel Chem. Prepr.-Am. Chem. Soc.* 50 (2) (2005) 435.
- [18] A.H. Cowley (Ed.), *Inorganic Syntheses*, Wiley, 1996.
- [19] G. Brauer, *Handbook of Preparative Inorganic Chemistry*, Academic Press, New York, 1963–1965.
- [20] G.M. Brown, M.-R. Noe-Spirlet, W.R. Busing, H.A. Levy, *Acta Cryst. B* 33 (4) (1977) 1038.
- [21] M.A. Sweikart, A.M. Herring, J.A. Turner, D.L. Williamson, B.D. McCloskey, S.R. Boonrueng, M. Sanchez, *J. Electrochem. Soc.* 152 (1) (2005) A98.
- [22] D.A. Boysen, T. Uda, C.R.I. Chisholm, S.M. Haile, *Science* 303 (5654) (2004) 68.
- [23] M.-C. Kuo, R.J. Stanis, J.R. Ferrell III, J.A. Turner, A.M. Herring, *Electrochim. Acta* 52 (2007) 2057.
- [24] B.R. Limoges, R.J. Stanis, J.A. Turner, A.M. Herring, *Electrochim. Acta* 50 (5) (2005) 1169.
- [25] G.M. Haugman, F. Meng, M.H. Frey, S.J. Hamrock, N. Aieta, J. Horan, M.C. Kuo, A.M. Herring, *Electrochem. Solid State Lett.* 10 (3) (2007) B51.
- [26] D.R. Vernon, F. Meng, S.F. Dec, D.L. Williamson, J.A. Turner, A.M. Herring, *J. Power Sources* 139 (1–2) (2005) 141.
- [27] P. Staiti, S. Hocevar, E. Passalacqua, *J. Power Sources* 65 (1–2) (1997) 281.